Biosensors and Bioelectronics 77 (2016) 202–207

Contents lists available at ScienceDirect

Biosensors and Bioelectronics

journal homepage: www.elsevier.com/locate/bios

A novel label-free electrochemical miRNA biosensor using methylene blue as redox indicator: application to breast cancer biomarker miRNA-21

Hossain-Ali Rafiee-Pour [a,*], Mohsen Behpour [b], Mahin Keshavarz [b]

[a] Biotechnology Division, Department of Molecular and Cell Biology, Faculty of Chemistry, University of Kashan, Kashan, Iran
[b] Department of Analytical Chemistry, Faculty of Chemistry, University of Kashan, Kashan, Iran

ARTICLE INFO

Article history:
Received 6 July 2015
Received in revised form
3 September 2015
Accepted 10 September 2015
Available online 16 September 2015

Keywords:
MicroRNA-21
Cancer detection
Electrochemical biosensor
Methylene blue
Label-free

ABSTRACT

Small noncoding microRNAs (miRNAs) have emerged as ideal noninvasive biomarkers for early-phase cancer detection. In this report, a label-free and simple electrochemical miRNA biosensor is developed based on employing methylene blue (MB) as a redox indicator. The successfully immobilization of the single strand DNA (ss-DNA) probe and hybridization with the target miRNA sequence were confirmed by electrochemical impedance spectroscopy (EIS) and cyclic voltammetry (CV) methods. Differential pulse voltammetry (DPV) technique was used to record the oxidation peak current of MB under optimal condition and an increase in the peak current was observed after hybridization. By employing this strategy, miRNA can detect in a range from 0.1 to 500.0 pM with a relatively low detection limit of 84.3 fM. The electrochemical response of MB on ss-DNA and duplex of miRNA/DNA was characterized by CV and chronocoulometry method. The linear relation between the redox peak currents (I_p) and scan rate (ν) indicates that the electron transfer (ET) between MB and the electrode surface was mediated by the miRNA/DNA π-stacked duplex. The value of surface coverage (Γ) was calculated that indicated increase amount of MB on the surface of modified electrode after hybridization event and revealed the adsorption of MB at modified electrode is monolayer. Also, the electron transfer rate constants (k_s) of MB were estimated. The results of kinetic analysis were confirmed by chronocoulometry method. The discrimination ability of miRNA biosensor even against a noncomplementary target was also studied. Consequently, this strategy will be valuable for sensitive, selective and label-free detection of miRNA.

© 2015 Elsevier B.V. All rights reserved.

1. Introduction

Cancer is a class of diseases characterized by out-of-control cell growth. Cancers can be source of serious disease and death. The most important challenge in cancer treatment is detection particularly at an early stage that could seriously decrease the universal health burden of cancer and save millions of lives. However, development of non-invasive or minimally invasive tests for detection of cancer remains an urgently challenge.

MicroRNAs (miRNAs) are small non-coding regulatory RNAs of 19–23 nucleotides which play vital role in the various physiological processes such as cell development, differentiation and immune system (Dong et al., 2013). Some advantages of miRNAs such as very accessible, low invasive and easily testable which makes them ideal biomarkers for clinical diagnosis (Yu et al., 2011). The selective releases of miRNAs from certain kind of malignant cells and specific altered miRNA expression might be applied for tumors classification (Lu et al., 2005; Peng et al., 2009). For instance, the circulating level of miRNA-21 was considerably higher in plasma specimens of breast cancer patients compared with in healthy controls (Kumar et al., 2013). Thus miRNA-21 could be used as diagnostic biomarkers for breast cancer screening and disease progression (Asaga et al., 2011).

Biosensors were designed for detection of wide variety of biomarkers from particular proteins, nucleic acid, to other metabolic or biological components. The biosensors made available possibility measurement of DNA or RNA fragments for early cancer detection. The various biosensor-based miRNA detection was reviewed in recent years (Johnson and Mutharasan, 2014; Keshavarz et al., 2015). A wide variety of platforms have been proposed for electrochemical determination of miRNA based on hybridization (Teo et al., 2014). The hybridization event is distinguished via change in current signal of a nucleic acid which resulted from hybridization (Lusi et al., 2009) or from variations in electrochemical parameters such as capacitance or resistance (Gao et al., 2013; Ren et al., 2013; Shen et al., 2013). Oligonucleotides labeled

* Corresponding author. Fax: +98 31 55912595.
E-mail address: rafieepour@kashanu.ac.ir (H.-A. Rafiee-Pour).

http://dx.doi.org/10.1016/j.bios.2015.09.025
0956-5663/© 2015 Elsevier B.V. All rights reserved.

with enzymes have mostly been employed in electrochemical biosensors to enhance sensitivity of miRNA detection (Zhou et al., 2012; Meng et al., 2013; Liu et al., 2014; Peng et al., 2014; Wu et al., 2015). Nevertheless, some of these approaches involve expensive materials or instruments, extremely time consuming and laborious experiment procedures. Consequently, there is an urgent demand for a new class of miRNA sensors that is simple, inexpensive, rapid and cost-effective platform enough to be used directly in clinical samples.

An attractive electrochemical hybridization assay for detection of nucleic acids is based on employing a redox indicator. The redox molecules show different electrochemical behaviors on single strands DNA (ss-DNA) or double strand DNA (ds-DNA) modified electrodes. Consequently, an alteration in the redox peak current can be used to monitor the hybridization event. A label-free electrochemical sensor was reported based on ferrocene boronic acid as redox probe for miRNA detection (Xia et al., 2013).

Methylene blue (MB) is an aromatic heterocyclic dye which interacts with nucleic acid sequence and can be employed as hybridization indicator to design of electrochemical nucleic acid biosensor (Erdem et al., 2001). The behavior of MB linked to single- and double-stranded oligonucleotides has been studied by both spectroscopy (Li et al., 2000; Vardevanyan et al., 2013) and electrochemistry (Kelley et al., 1997) methods. The possible mechanism of interaction have been established either via guanine bases present at ss-DNA (Yang et al., 2002), electrostatic interaction with negatively charged backbone phosphate groups (Zhao et al., 1999), or direct intercalation between guanine–cytosine pairs in the DNA double helix (Arias et al., 2009). Depending on the binding mode of MB-DNA complex, both an decrease (Zhu et al., 2004; Zhang et al., 2008) or increase (Sun et al., 2010) in the voltammetric response after hybridization were reported for quantification of nucleic acid sequences. Recently, Gooding et al. demonstrated the ability of MB for detection of DNA and miRNA target (Tavallaie et al., 2014).

In this work, a convenient and label-free platform for sensitive detection of miRNAs was presented based on MB as a hybridization indicator. The difference between the oxidation peak current of MB on DNA or duplex DNA/miRNA was employed for determination of miRNA-21 concentration. The main advantage of our work is that miRNA can be determined without any laborious labeling and operation complexity.

2. Experimental

2.1. Chemicals and materials

Synthetic capture probes ss-DNA and miRNA sequences used in this work were purchased from Bioneer Corporation (South Korea). The oligonucleotide sequences are listed in Table S1 (see supporting information). All chemicals that used were purchased from Merck and were used without further purification. The buffer solutions used in this work are as follows. Buffer for ss-DNA immobilization was 10 mM K_2HPO_4-citric acid containing 1.0 M NaCl (pH 5.4). Hybridization buffer was prepared with 1.0 × SSC (Saline-Sodium Citrate) solution containing 15 mM tri-sodium citrate and 150 mM NaCl. Washing buffer solution was 0.1 × SSC. A pH 7.4 phosphate-buffer solution (PBS, 20 mM phosphate buffer + 0.15 M NaCl) was used as the supporting electrolyte for differential pulse voltammetry (DPV) quantification. All solutions were treated with diethyl pyrocarbonate (DEPC) and all sample tubes, microtips and glassware autoclaved to minimize the effect of RNases on the stability of miRNAs. MWCNTs with lengths of 50 μm was purchased from Times Nano Company (Chengdu, China) and were applied without additional purification.

2.2. Apparatus

Electrochemical experiments were carried out with an Autolab system (model PGSTAT30). A conventional three-electrode system, consisting of a 1.0-mm diameter glassy carbon electrode (GCE), an Ag/AgCl (3.0 M KCl) reference electrode and a platinum wire counter electrode were used in all electrochemical measurements. The used electrochemical techniques are cyclic voltammetry (CV), electrochemical impedance spectroscopy (EIS), differential pulse voltammetry (DPV), and chronocoulometry. EIS experiments were performed in 5.0 mM $K_3Fe(CN)_6/K_4Fe(CN)_6$ containing 0.10 M KCl, over a frequency range from 1.0 MHz to 0.1 Hz with a AC voltage amplitude 0.05 V and a bias potential of 0.2 V. All experimental results were fitted to a Randle's equivalent circuit, using NOVA software, which allowed extracting the resistance. An Eurosonic 4D ultrasonic water bath with a digital timer and a temperature control was applied for dispersion (Euronda, Montecchio Precalcino (Vincenza) Italy).

2.3. Fabrication of electrochemical miRNA biosensor

Firstly, a GCE was thoroughly polished with 5.0 and 0.5 μm alumina slurry, respectively. Then GCE was sonicated in mixture of ethanol/water for 5 min. MWCNT-COOH was prepared according to the literature (Karimi et al., 2012). In a typical procedure, 20 mg of MWCNTs were dispersed in 30 mL nitric acid solution (35%) by ultrasonic bath for 3 h. After that, the black suspension was filtered with vacuum filtration equipped poly tetra fluoro ethylene (PTFE) membrane (pore size 0.45 μm) and washed thoroughly with distilled water until neutral pH and then dried under the infrared lamp. MWCNT-COOH was dispersed into DMF (4 mg mL^{-1}) to provide a black suspension. Next, 2.5 μL suspension of MWCNT-COOH was dropped on the cleaned GCE and allowed to dry at room temperature. Subsequently, the capture probe adsorption was accomplished by immersing MWCNT-COOH modified GCE (MWCNT-COOH/GCE) into 200 μL immobilization buffer (pH 5.4) containing 1.0 μM ss-DNA (as capture probe) at room temperature for 120 min. After the adsorption, the modified electrode (ss-DNA/MWCNT-COOH/GCE) was gently rinsed with PBS to remove unbound ss-DNA probe. Then, half of the ss-DNA immobilized electrodes was incubated in 1.0 × SSC containing the target miRNA (miRNA-21) for 1.0 h to achieve hybridization (miRNA/ss-DNA/MWCNT-COOH/GCE). The non-hybridizated adsorbed miRNA could be removed from the biosensor surface when exposed to 0.1 × SSC. The ss-DNA/MWCNT-COOH/GCE and miRNA/ss-DNA/MWCNT-COOH/GCE was immersed into MB solution (4.0 μM MB–0.2 M NaCl–0.10 M PBS pH 7.4) for 5 min. The modified electrodes was then rinsed carefully with PBS to remove any excess of MB in order to ensure that the electrochemical signal obtained only accounts for MB bound to the sequences. Finally, the MB oxidation current was measured by DPV in PBS (pH 7.4). The electrochemical signal of MB was compared before and after hybridization and the significant increase in peak current attributes to target miRNA concentration. The analysis principle of the label-free electrochemical miRNA biosensor is depicted in Scheme 1.

3. Results and discussion

3.1. Electrochemical characterization of modified electrodes

EIS is a convenient and effective tool to provide important information about the impedance varies of the substrate surface during the electrode modification process. The Nyquist plot is a typical impedance spectrum which displays two semicircular and linear portions at higher and lower frequencies, respectively. The

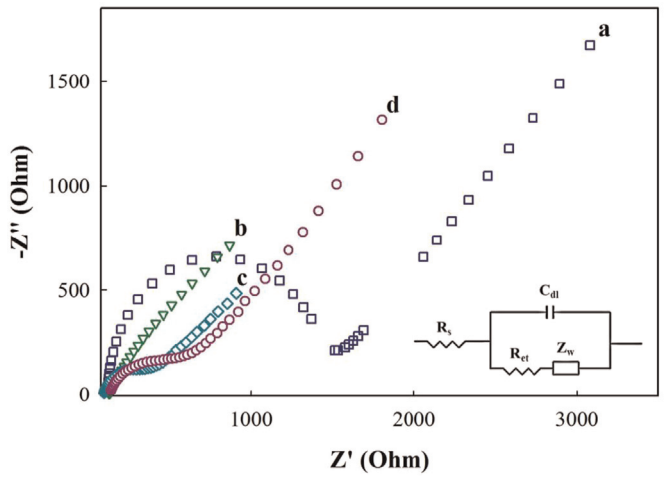

Fig. 1. Nyquist diagram of electrochemical impedance spectra recorded in 5.0 mM $[Fe(CN)_6]^{3-/4-}$ solution containing 1.0 M KCl using: (a) GCE, (b) MWCNT/GCE, (c) ss-DNA/MWCNT-COOH/GCE, and (d) miRNA/ss-DNA/MWCNT-COOH/GCE. The inset displays the Randles circuit to fit the experimental EIS data.

diameter of semicircular portion corresponds to the electron transfer resistance (R_{et}), whereas the linear part corresponds to the lower frequency regimes where the electrochemical process is under mass transfer control (Bard and Faulkner, 2001). The Nyquist plot of different electrodes was recorded to reveal the stepwise assembly of ss-DNA and miRNA-21 on the surface of modified electrode as shown in Fig. 1. The bare GCE demonstrated a larger semicircle, showing resistance towards the electron transfer (ET) process on the GCE (Fig. 1a). As can be seen in Fig. 1b, the MWCNT-COOH/GCE exhibits no semicircle domain and only an almost straight line, reflecting excellent electron conduction ways between redox probes ($[Fe(CN)_6]^{3-/4-}$) and the modified electrode surface. It should be attributed to the excellent conductivity of MWCNTs-COOH (Fig. 1b). After immobilization of ss-DNA (named as ss-DNA/MWCNT-COOH/GCE), the R_{et} value further increased which revealed that ss-DNA had been successfully immobilized on the modified electrode surface (Fig. 1c). The ss-DNA sequences are attached to MWCNT-COOH/GCE via amid covalent bond formation between amino group in ss-DNA and carboxylic acid group of MWCNT-COOH (Kilic et al., 2012). This increase in R_{et} value can be explained by the fact that immobilized DNA molecules serves as a blocking layer that reduce effective area t ET due to increase in the thickness of interface (Ferreira et al., 2010). Also, this monolayer prevented access of the redox probe to the modified electrode surface because of the electrostatic repulsion between negative charged of the ss-DNA phosphate skeletons and the negatively charged $[Fe(CN)_6]^{3-/4-}$ ions (Shamsi and Kraatz, 2011). The larger semicircle was observed after ss-DNA hybridized with miRNA-21 (named as miRNA/ss-DNA/MWCNT-COOH/GCE) which suggested a slow electron transfer rate (Fig. 1d). This phenomenon can be illuminated by the fact that the negatively charged backbone of target miRNA causing increased negative charges of the surface, so amplified repulsive forces to the $[Fe(CN)_6]^{3-/4-}$ ions. The increased R_{et} value attributed to the hybridization between ss-DNA and miRNA. Thus, the successfully fabrication of biosensor have been confirmed by EIS results.

CV is one of the most popular electrochemical methods and is often used for attaining information about electrochemical processes taking place at electrode-solution interface. The hybridization process between ss-DNA capture probes and the target miRNA was further confirmed by CV in 5.0 mM $[Fe(CN)_6]^{3-/4-}$ solution containing 0.10 M KCl, which was displayed in Fig. 2A. The cyclic voltammogram of MWCNT-COOH/GCE exhibits in curve a. A decrease in peaks current appeared for ss-DNA/MWCNT-COOH/GCE

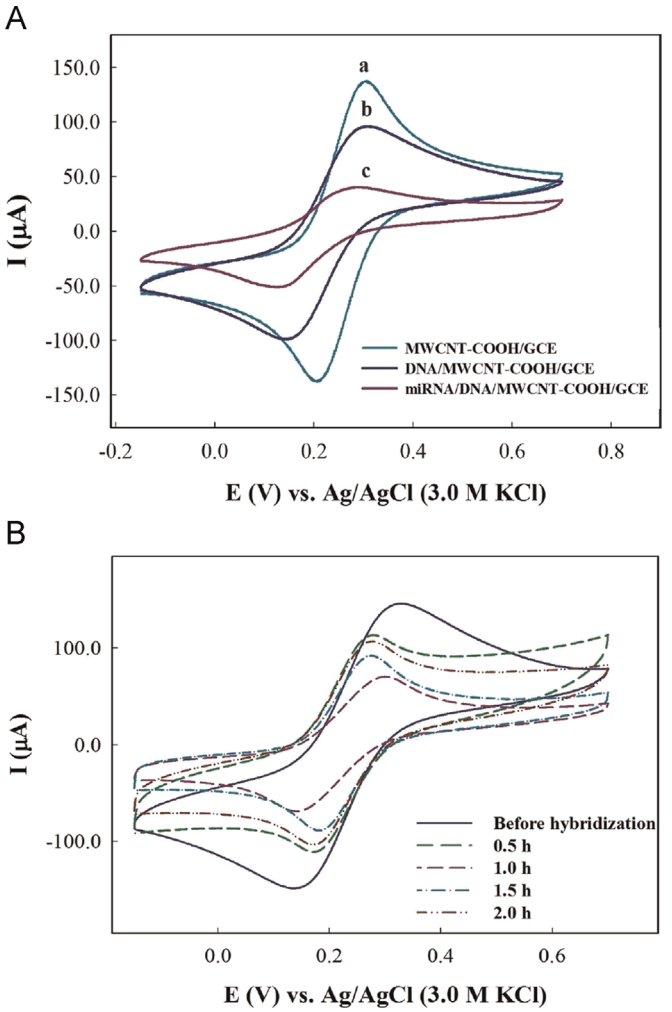

Fig. 2. (A) Cyclic voltammograms carried out in 5.0 mM $[Fe(CN)_6]^{3-/4-}$ solution containing 1.0 M KCl for (a) MWCNT-COOH/GCE, (b) ss-DNA/MWCNT-COOH/GCE, and (c) after incubation in 100.0 pM miRNA-21 with a scan rate 0.1 V s^{-1}. (B) Cyclic voltammograms recorded in 5.0 mM $[Fe(CN)_6]^{3-/4-}$ solution containing 1.0 M KCl for ss-DNA/MWCNT-COOH/GCE incubated within 100.0 pM miRNA-21 solution in different times (scan rate 0.1 V s^{-1}).

(curve b). The immobilized ss-DNA could act as blocking electron transfer between redox probe and the electrode surface. It could be easily seen that the redox peak current was reduced significantly when the modified electrode incubated in the target miRNA solution (curve c). Hybridization with the target miRNA may decrease conductivity and the efficiency of ET between electrode and redox probes. So, this decrease in peaks current could be attributed to successfully hybridization of miRNA with ss-DNA.

3.2. Optimization of hybridization time

A key issue with nucleic acid hybridization biosensor is hybridization time. The influence of hybridization time was assessed for optimum analytical performance. The ss-DNA/MWCNT-COOH/GCE was incubated within 100.0 pM miRNA-21 solution for 0.5, 1.0, 1.5 and 2.0 h, and the cyclic voltammograms recorded are presented in Fig. 2B. The redox peak currents of the miRNA modified electrode decreased after 0.5 h treated on miRNA-21 solution that indicated the ss-DNA/miRNA duplex acts as mass transfer blocking layer and consequently hinders the diffusion of $[Fe(CN)_6]^{3-/4-}$ ions toward the surface of electrode. The reducing peak current reached a maximum following an extended exposure

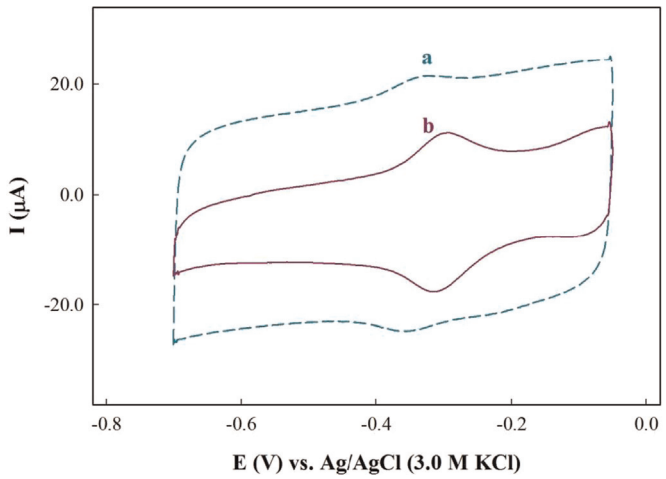

Fig. 3. Representative cyclic voltammograms recorded in 0.2 M PBS containing 0.15 M NaCl at pH 7.4 for (a) ss-DNA/MWCNT-COOH/GCE and (b) miRNA/ss-DNA/MWCNT-COOH/GCE after incubation with 4.0 μM MB solution for 5 min. The scan rate was 0.1 V s^{-1}.

to 1.0 h and then the peak current increased due to the strict effect for hybridization events (Mashhadizadeh and Pourtaghavi Talemi, 2014). Therefore, these results suggested the hybridization reaction was completed after 1.0 h and this value was chosen and adopted in the following work.

3.3. Study of MB binding

MB was applied as an electrochemical indicator to investigate the hybridization with the target miRNA sequence. MB reduce to leucomethylene blue with a quasi-reversible two electrons and one proton reaction at physiological pH (Ju et al., 1995). The planar heterocyclic dye is probable to stabilize its binding to DNA through favorable stacking interactions with its adjacent base pairs (Nafisi et al., 2007). The electrochemical signal of MB can be change after the hybridization event on the electrode surface, due to the different affinity of MB for single and double strand nucleic acid sequence. This redox signal variation can be exploited for development of miRNA biosensors based MB as a redox indicator. Typical cyclic voltammograms from each of the modified electrodes recorded after incubated with MB solution for 5 min (Fig. 3). The redox signals are because of the ET reaction between the bounded MB and the surface of electrode. The amount of accumulated MB molecules on the surface of electrode increased after hybridization. It is known that for short-length DNA hybrid, the electrochemical response from MB bound increase due to increase amount of MB molecules bound and they are available for ET reaction with the surface of electrode. For longer DNA hybrid, a part of the MB molecules bound seem to be electrochemically unreadable due to long ET distance (Farjami et al., 2010). In this work, the short sequences were applied, so we expected that the electrochemical signal of MB bound increase after duplex formation. Compared to ss-DNA/MWCNT-COOH/GCE (Fig. 3a), an increase in the anodic and cathodic peak current was found after hybridization process (Fig. 3b). These increase in peak currents after hybridization revealed more accumulated MB molecules on the surface. Thus, the increase in the current magnitude confirmed the hybridization existence at the surface of electrode.

The reduction peak potential (E_{pc}) were −0.356 and −0.304 V for MB-ss-DNA/MWCNT-COOH/GCE and MB-miRNA/ss-DNA/MWCNT-COOH/GCE, respectively. The E_{pc} of MB after hybridization was shifted positively values compared to MB-ss-DNA/MWCNT-COOH/GCE. These shifts likely reflecting the different environment located MB and also suggested that MB binds to miRNA/DNA more than to ss-DNA (Pan et al., 2007).

3.3.1. Kinetic analysis

The binding of MB to duplex strands can take place via intercalative or groove binding (Nafisi et al., 2007). The orientation of MB binding to DNA sequences was interpreted (Rohs and Sklenar, 2004). The mode of interaction MB with nucleic acid strongly depends on the experimental conditions such as ionic strength of MB solution. The orientation of the MB long axis to be parallel to the averaged long axis of the two base pairs at low salt, variations to a perpendicular orientation in the case of high salt concentration (Rohs et al., 2000). The spectroscopic data clearly indicated that the binding mode for the GC polynucleotide $[poly(dG\text{-}dC)]_2$ is only intercalative. But binding of MB to the alternating AT polynucleotide $[poly(dA\text{-}dT)]_2$ is mainly intercalative at low ionic strength but groove-binding is also manifest at high ionic strength (0.2 M PBS) (Tuite and Norden, 1994). Consequently, we expect that MB binding is taking place via intercalation under our experimental conditions.

The ET between MB and the surface of electrode occurs through directional or miRNA/DNA-mediated (Scheme S1: A and B, respectively). It is apparent that ET was mediated by the hybrid helix only when the MB molecules are bound to hybrid duplex by intercalation. The redox peak currents (I_p) are linearly proportional to the scan rate (ν) (Fig. S2), indicating that the ET between MB and the modified electrode surface was mediated by the miRNA/DNA π-stacked duplex (Farjami et al., 2011). So these result shows MB can take place within intercalative of hybridized duplex. Our assumption is in contrast with the results obtained in this study.

The linearly dependence of I_p on ν displays a surface-confined ET process. The surface coverage of MB-DNA (Γ_{DNA}) or MB-miRNA/DNA ($\Gamma_{miRNA/DNA}$) can be estimated by followed equation (Bard and Faulkner, 2001):

$$I_p = (9.39 \times 10^5)\, n^2 A \Gamma \nu \quad (1)$$

where n is the number of electrons involved in the electrode reaction ($n=2$ for MB) (Ju et al., 1995), A the electrode surface area (cm^2). The value of Γ_{DNA} and $\Gamma_{miRNA/DNA}$ was calculated 130.83 and 507.46 (pmol cm^{-2}), respectively. These results being a good agreement with the increase amount of MB on the surface of modified electrode after hybridization event.

The theoretical surface coverage (Γ_{theory}) of monolayer absorbance of MB at the surface of electrode is 220 (p mol cm^{-2}) (Ju et al., 1995). So the ratio of Γ to Γ_{theory} ($\eta=\Gamma/\Gamma_{theory}$) was obtained 0.60 and 2.31 for MB-DNA and MB-miRNA/DNA modified electrode, respectively. The value of η after hybridization is larger than the theoretical value due to the increase in the electrode surface roughness. The η value is just close to the value that shows the adsorption of MB at the modified electrode is monolayer (Ju et al., 1995).

The oxidation peak potential (E_{pa}) shifts to positive value with increasing scan rate (>1 V s^{-1}) and the E_{pc} also shifts to more negative values. The difference between the cathodic and the anodic peak potential (ΔE_p) increased with increasing ν that reflect the rate of heterogeneous ET reactions of the MB in the monolayer.

The electron transfer rate constant (k_s) of MB for both ss-DNA/MWCNT-COOH/GCE and miRNA/ss-DNA/MWCNT-COOH/GCE were estimated by Laviron analysis (Laviron, 1979). A graph of ΔE_p versus log ν gives a straight line when ΔE_p values are more than 200/n mV. The electron transfer coefficient (α) and k_s can be calculated from the help of slope and intercept of straight line, respectively. The k_s value for ss-DNA/MWCNT-COOH/GCE before and after hybridization was obtained 5.61 ± 0.33 and 4.40 ± 0.21 s^{-1}, respectively. This was reported that the k_s value is between 1.5–

40 s^{-1} when DNA meditated ET (Farjami et al., 2012), so the ET between MB molecules and the electrode surface was meditated by ss-DNA and miRNA/DNA duplex.

The difference in the k_s value is attributed to the varies distance between the electrode surface and the redox indicator (Smalley et al., 1995). Here the difference in the k_s value indicate that the average distance between MB and MWCNT-COOH/GCE surface significantly increased in the hybridized state that owing to the greater rigidity of the double-stranded probe compared to that of the single-stranded probe (Yang and Lai, 2011). The electron-transfer kinetics study provides further information about the hybridization formation at the surface of modified electrode.

3.3.2. Chronocoulometric study

Chronocoulometry is a promising potential step method for measurement of electroactive molecules adsorbed on the electrode surface. The charge (Q) for electroreduction of surface-adsorbed electroactive species is given by:

$$Q = Q_{dl} + nFA\Gamma \quad (2)$$

where, Q_{dl} is double-layer charging that can be evaluated in the absence of adsorbed redox species, Γ is the surface coverage of electroactive species (mol cm^{-2}) and other symbols have their usual meaning.

The Q increased with the increasing of the MB concentration and reached a maximum value. The plot of Q versus MB concentration was shown in the Fig. S3, which exhibited an expected shape of Langmuir adsorption (Kara et al., 2002). According to the Langmuir adsorption thermodynamic equation:

$$\frac{[MB]}{Q} = \frac{1}{\Gamma_{max}K} + \frac{[MB]}{\Gamma_{max}} \quad (3)$$

where Q represents coulometric charge, Γ_{max} the maximum number of MB binding sites, [MB] the concentration of MB and K the adsorption constant of MB on the modified electrode. From the slope and the intercept of the plot of [MB]/Q vs. [MB], the Γ_{max} and K value can be obtained (Fig. S4). The good correlation coefficients (R^2=0.9895 and 0.9996) indicate that the Langmuir model acceptably fits the experimental results. The value of Γ_{max} and K are presented in Table S2. An increase in K value after hybridization showed that the MB had stronger affinity with miRNA/DNA than ss-DNA and the complex of MB with miRNA/DNA duplex was more stable than MB with ss-DNA (Zhu et al., 2008). A high dye binding (Γ_{max}) was observed for miRNA/DNA duplex confirmed the pervious tendencies observed in the kinetic analysis.

3.4. Performance of the designed biosensor for miRNA-21quantitative detection

DPV is found to be a sensitive electrochemical technique and is widely applied to analytical purposes. In this work, DPV revealed variations of the electrochemical response of MB after hybridization of ss-DNA capture probe with miRNA target (Fig. 4A). The peak current was attributed to the oxidation of MB on ss-DNA/MWCNT-COOH/GCE (curve a) and miRNA/ss-DNA/MWCNT-COOH/GCE (curve b), respectively. The oxidation current of MB after hybridization with the target miRNA was 1.48 times higher than before hybridization event. The distinction between the oxidation currents for MB bonded to DNA and miRNA/DNA systems is sufficient for quantitation of miRNA detection. This current difference (ΔI) measured for different miRNA concentration is presented as calibration curve in Fig. 4B. At least three replicates were performed for each miRNA concentration to attain a calibration curve. The ΔI is linearly correlation versus the logarithmic of miRNA concentration in a range from 0.1 to 500.0 pM with the regression

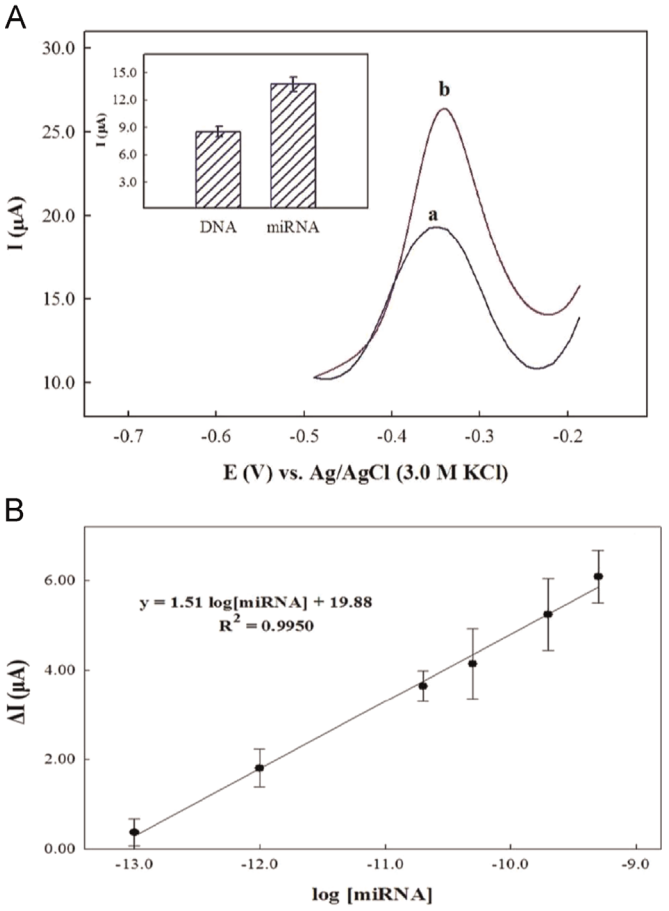

Fig. 4. (A) DPV curves for oxidation of MB at (a) DNA/MWCNT-COOH/GCE (E_{pa} = −0.338), and (b) miRNA/ss-DNA/MWCNT-COOH/GCE (E_{pa} = −0.358). Insets: Histograms with error bars of MB oxidation signals. **(B)** Relationship between ΔI and logarithm of miRNA-21 concentration. Data points represented three replicates.

equation of ΔI = 1.51 log C + 19.88 (I is the peak current and C is the miRNA concentration, R^2=0.9950). The detection limit was estimated to be 84.3 fM (n=3). The relative standard deviations (RSDs) are all less than 7.7% indicating that multiple electrodes can be prepared simultaneously for the samples assays.

3.5. Selectivity

The biosensor capability in selectivity detection of specific miRNAs is an important attention. The selectivity of the proposed miRNA biosensor was investigated by a comparison study on perfect complementary target and mismatch target. As expected, the electrochemical signal for complementary target miRNA-21 was higher than the current of non-complementary sequence (miRNA-192) at a same concentration of 200.0 pM (Fig. 5). This current decrease corresponds to the prevention of direct ET through the duplex in the presence of a non-complementary target. This result demonstrates that the proposed biosensor is selective for discrimination complementary miRNA-21 from miRNA-192 and this non-complementary sequence could not influence the accuracy determination of miRNA-21 in real samples.

4. Conclusion

The present study demonstrated a label-free electrochemical biosensor for detection of miRNA-21 as a model to detect of breast

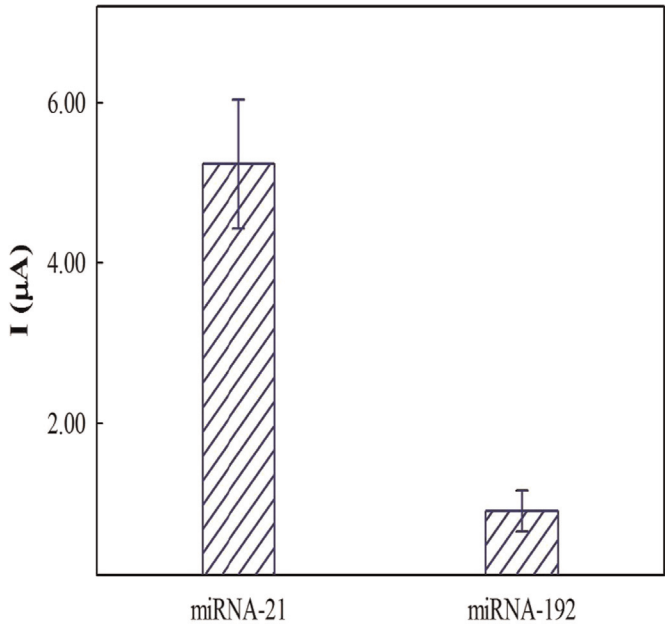

Fig. 5. DPV responses of a miRNA biosensor to 200.0 pM of miRNA-21 and miRNA-192. Error bars were related to three independent measurements.

cancer. The difference of MB electrochemical response on ss-DNA immobilized modified electrodes before and after hybridization event was applied for specific detection of miRNA-21. This approach achieved a linear range from 0.1 to 500.0 pM with a detection limit of 84.3 fM by DPV method. The proposed assay obviates the use of any label for ss-DNA or miRNA, enzyme, complexity process or expensive bioreagents so this procedure is significantly simplified. The results indicated that this electrochemical miRNA biosensor presented the notable advantages such as low-cost simple preparation procedure, relatively fast and wider linear range. We believe that the designed biosensor can serve as an attractive candidate for sensitive and selective determination of miRNAs in biological samples, which may be has fine adaptability to the applications in cancer detection.

In addition, we studied MB binding by CV and chronocoulometry method. The kinetic analysis demonstrated that MB binding is taking place via intercalation under our experimental conditions and the adsorption of MB at modified electrode is monolayer. The difference in value of k_s after hybridization was ascribed to the variation distance between the electrode surface and the redox indicator. The electron-transfer kinetics study provides further information about the hybridization formation at the surface of modified electrode. The increase of K value after hybridization showed that the MB had stronger affinity with miRNA/DNA than ss-DNA and the complex of MB with miRNA/DNA duplex was more stable than MB with ss-DNA.

Acknowledgment

The authors wish to express their gratitude to University of Kashan for supporting this work by Grant No 463561-5.

Appendix A. Supplementary material

Supplementary material associated with this article can be found in the online version at http://dx.doi.org/10.1016/j.bios.2015.09.025.

References

Arias, P., Ferreyra, N.F., Rivas, G.A., Bollo, S., 2009. J. Electroanal. Chem. 634, 123–126.
Asaga, S., Kuo, C., Nguyen, T., Terpenning, M., Giuliano, A.E., Hoon, D.S.B., 2011. Clin. Chem. 57, 84–91.
Bard, A.J., Faulkner, L.R., 2001. Electrochemical Methods: Fundamentals and Applications, second ed. Wiley, New York.
Dong, H., Lei, J., Ding, L., Wen, Y., Ju, H., Zhang, X., 2013. Chem. Rev. 113, 6207–6233.
Erdem, A., Kerman, K., Meric, B., Ozsoz, M., 2001. Electroanalysis 13, 219–223.
Farjami, E., Campos, R., Ferapontova, E.E., 2012. Langmuir 28 16218–1626.
Farjami, E., Clima, L., Gothelf, K., Ferapontova, E.E., 2011. Anal. Chem. 83, 1594–1602.
Farjami, E., Clima, L., Gothelf, K.V., Ferapontova, E.E., 2010. Analyst 135, 1443–1448.
Ferreira, D.C.M., Mendes, R.K., Kubota, L.T., 2010. J. Braz. Chem. Soc. 21, 1648–1655.
Gao, Z., Deng, H., Shen, W., Ren, Y., 2013. Anal. Chem. 85, 1624–1630.
Johnson, B.N., Mutharasan, R., 2014. Analyst 139, 1576–1588.
Ju, H., Zhou, J., Cai, C., Chen, H., 1995. Electroanalysis 7, 1165–1170.
Kara, P., Kerman, K., Ozkan, D., Meric, B., Erdem, A., Ozkan, Z., Ozsoz, M., 2002. Electrochem. Commun. 4, 705–709.
Karimi, S., Ghourchian, H., Rahimi, P., Rafiee-Pour, H.A., 2012. Anal. Methods 4, 3225–3231.
Kelley, S.O., Barton, J.K., Jackson, N.M., Hill, M.G., 1997. Bioconjugate Chem. 8, 31–37.
Keshavarz, M., Behpour, M., Rafiee-pour, H.-A., 2015. RSC Adv. 5, 35651–35660.
Kilic, T., Nur, S., Ozkan, D., Ozsoz, M., 2012. Biosens. Bioelectron. 38, 195–201.
Kumar, S., Keerthana, R., Pazhanimuthu, A., Perumal, P., 2013. Indian J. Biochem. Biophys. 50, 210–214.
Laviron, E., 1979. J. Electroanal. Chem. 101, 19–28.
Li, W., Xu, J., He, X., 2000. Anal. Lett. 33, 2453–2464.
Liu, L., Xia, N., Liu, H., Kang, X., Liu, X., Xue, C., 2014. Biosens. Bioelectron. 53, 399–405.
Lu, J., Getz, G., Miska, E.A., Alvarez-Saavedra, E., Lamb, J., Peck, D., Sweet-Cordero, A., Ebert, B.L., Mak, R.H., Ferrando, A., Downing, A., Jacks, J.R., Horvitz, T., Golub, T. R., H.R., 2005. Nature 435, 834–838.
Lusi, E.A., Passamano, M., Guarascio, P., Scarpa, A., Schiavo, L., 2009. Anal. Chem. 81, 2819–2822.
Mashhadizadeh, M.H., Pourtaghavi Talemi, R., 2014. Anal. Methods 6, 8956–8964.
Meng, X., Zhou, Y., Liang, Q., Qu, X., Yang, Q., Yin, H., Ai, S., 2013. Analyst 138, 3409–3415.
Nafisi, S., Saboury, A.A., Keramat, N., Neault, J.F., Tajmir-Riahi, H.A., 2007. J. Mol. Struct. 827, 35–43.
Pan, D., Zuo, X., Wan, Y., Wang, L., Zhang, J., Song, S., Fan, C., 2007. Sensors 7, 2671–2680.
Peng, S., Zeng, X., Li, X., Peng, X., Chen, L., 2009. J. Genet. Genom. 36, 409–416.
Peng, Y., Jiang, J., Yu, R., 2014. Anal. Methods 6, 2889–2893.
Ren, Y., Deng, H., Shen, W., Gao, Z., 2013. Anal. Chem. 85, 4784–4789.
Rohs, R., Sklenar, H., 2004. J. Biomol. Struct. Dyn. 21, 699–711.
Rohs, R., Sklenar, H., Lavery, R., Roder, B., 2000. J. Am. Chem. Soc. 122, 2860–2866.
Shamsi, M.H., Kraatz, H.B., 2011. Analyst 136, 3107–3112.
Shen, W., Deng, H., Ren, Y., Gao, Z., 2013. Biosens. Bioelectron. 44, 171–176.
Smalley, J.F., Feldberg, S.W., Chidsey, C.E.D., Linford, M.R., Newton, M.D., Yi-ping, L., 1995. J. Phys. Chem. 99, 13141–13149.
Sun, W., Qin, P., Gao, H., Li, G., Jiao, K., 2010. Biosens. Bioelectron. 25, 1264–1270.
Tavallaie, R., Darwish, N., Gebala, M., Hibbert, D.B., Gooding, J.J., 2014. ChemElectroChem 1, 165–171.
Teo, A.K.L., Lim, C.L., Gao, Z., 2014. Electrochim. Acta 126, 19–30.
Tuite, E., Norden, B., 1994. J. Am. Chem. Soc. 116, 7548–7556.
Vardevanyan, P.O., Antonyan, A.P., Parsadanyan, M.A., Shahinyan, M.A., Hambardzumyan, L.A., 2013. J. Appl. Spectrosc. 80, 610–614.
Wu, X., Chai, Y., Zhang, P., Yuan, R., 2015. ACS Appl. Mater. Interfaces 7, 713–720.
Xia, N., Wang, X., Deng, D., Wang, G., Zhai, H., Li, S., 2013. Int. J. Electrochem. Sci. 8, 9714–9722.
Yang, W., Lai, R.Y., 2011. Langmuir 27, 14669–14677.
Yang, W., Ozsoz, M., Hibbert, D.B., Justin, J., 2002. Electroanalysis 14, 1299–1302.
Yu, D., Li, Q., Ding, X., Ding, Y., 2011. Int. J. Mol. Sci. 12, 2055–2063.
Zhang, W., Yang, T., Huang, D.M., Jiao, K., 2008. Chin. Chem. Lett. 19, 589–591.
Zhao, G., Zhu, J., Zhang, J., Chen, H., 1999. Anal. Chim. Acta 394, 337–344.
Zhou, Y., Zhang, Z., Xu, Z., Ai, S., 2012. New J. Chem. 36, 1985–1991.
Zhu, L., Zhao, R., Wang, K., Xiang, H., Shang, Z., Sun, W., 2008. Sensors 8, 5649–5660.
Zhu, N., Zhang, A., Wang, Q., He, P., Fang, Y., 2004. Anal. Chim. Acta 510, 163–168.